Journal of Mechatronics Engineering

Detection of Microcalcifications in Mammography using Image Processing

ADAILTON S. HOLANDA[1], JOSIAS G. BATISTA[1],
AUZUIR R. ALEXANDRIA[1]

[1]Industry Department, Federal Institute of Education, Science and Technology of Ceará, 2081 Treze de Maio Ave, 60040-215 Fortaleza, Brazil (IFCE)
<adailtondsh@gmail.com>, <josiasbatista@ifce.edu.br>,
<auzuir@ifce.edu.br>

DOI: 10.21439/jme.v8i1.115

Abstract. Breast cancer is the most diagnosed type of cancer and the one that causes the most deaths in women in the world. Mammography images allow the detection of microcalcifications at an early stage. This work aims to develop a computer vision system to detect microcalcifications in Mammography images. For this purpose, images from the Curated Breast Imaging Subset of Digital Database for Screening Mammography (CBIS-DDSM) database are used. The detection algorithm is divided into two parts: pre-processing and segmentation. A region of interest was not defined, as it is considered that the entire breast is subject to the appearance of microcalcifications. The programming language used was Python and the Numpy and OpenCV libraries. Accuracy, sensitivity, specificity, positive predictive value, and Dice Similarity were calculated for validation. The experiments show that the method's accuracy is 98.2%, the sensitivity is 49.6%, the specificity is 89.3%, the positive predictive value is 78.7%, and the Similarity Dice is 52.7%. The developed system achieved the desired objective with good performance.

Keywords: Detection of microcalcifications. Computer vision. Computer-assisted diagnosis.

(Received: October 26^{th}, 2024 / Accepted: September 23^{rd}, 2025)

1 Introduction

Breast cancer is the most diagnosed type of cancer and the one that causes the most deaths in women (SOCIETY, 2007). This occurs in both developed and developing countries (JEMAL et al., 2011). In Europe, breast cancer is the leading cause of death in women, causing one-sixth of all cancer deaths (MLADOVSKY, 2009). In the United States, a woman has a 12.15% chance of developing this type of cancer in her lifetime (SOCIETY, 2007).

Programs to encourage periodic mammography examinations in developed countries have been implemented (SOCIETY, 2007). In the United States, women aged 40 and over are encouraged to take the exam (NETWORK et al., 2007). In the United Kingdom, women aged between 50 and 70 are invited to undergo screening every three years (METZGER-FILHO et al., 2012).

Mammography is the preferred method for early detection of breast cancer, as well as being the most efficient and cost-effective. However, the task of identifying microcalcifications and classifying them as malignant or benign is not simple (CHEN et al., 2014). Due to the difficulty often encountered in providing an accurate diagnosis, computer-aided diagnosis (CAD) techniques are important to offer a second suggestion to radiologists in cases that are difficult to identify and conclude (DONG et al., 2015). An example of a Mammography image used in this work is shown in Figure 1.

Computer-aided diagnosis (CAD) systems have become an indispensable tool in modern medical practice, particularly in addressing challenges related to diagnostic accuracy. Radiologists often face difficulty interpre-

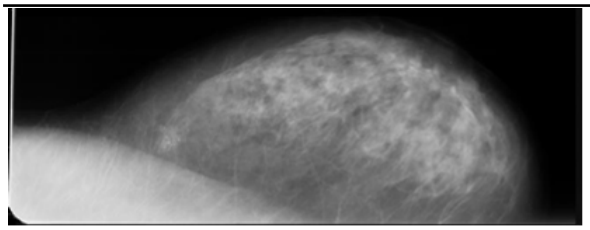

Figure 1: Example of Mammography image used in this work (Source: CBIS-DDSM dataset).

ting complex cases where subtle abnormalities may be missed or misdiagnosed. CAD systems offer a valuable second opinion, helping to enhance diagnostic accuracy, reduce human error, and improve patient outcomes (LI; NISHIKAWA, 2015).

By leveraging advanced algorithms and techniques such as image processing, machine learning, and deep learning, CAD systems analyze medical images like X-rays, CT scans, and MRIs to identify patterns indicative of diseases. For example, CAD systems are widely used in detecting early signs of breast cancer, lung nodules, and cardiovascular abnormalities. These tools act as supplementary aids to radiologists by providing consistent and repeatable evaluations, especially in cases where human interpretation may be subjective or influenced by fatigue (DIKICI et al., 2020).

Several studies have highlighted the effectiveness of CAD in improving diagnostic efficiency. For instance, integrating CAD with radiological workflows has been shown to increase the sensitivity of cancer detection without significantly compromising specificity. Advances in artificial intelligence (AI) have further enhanced CAD capabilities, enabling the detection of minute details that may be imperceptible to the human eye. These systems also facilitate personalized treatment planning by providing quantitative assessments and actionable insights (LITJENS et al., 2017).

Despite its benefits, CAD systems also have limitations, such as dependency on high-quality datasets for training, susceptibility to biases in the data, and challenges in integration with existing healthcare workflows. Nonetheless, continuous advancements in AI and imaging technologies hold promise for overcoming these challenges, further solidifying the role of CAD in healthcare (DOI, 2007).

Mammography images allow the detection of microcalcifications at an early stage. It is important to note that not all microcalcifications indicate the presence of cancer; only some groups with specific characteristics are associated with a high probability of being malignant (SICKLES, 1986). Many CAD techniques for microcalcifications in Mammography images have been presented. Various features have been studied in the literature to characterize and classify these abnormalities as malignant or benign. These characteristics are shape, morphology, group, brightness intensity, texture, etc. (CHEN et al., 2014).

Microcalcifications are tiny deposits of calcium salts within the breast tissue. On Mammography images, they appear as pixels with greater intensity (SHEN; RANGAYYAN; DESAUTELS, 1994). The presence of groups of microcalcification is one of the first signs of possible breast cancer. The radiological definition of a group of microcalcifications is a $1\ cm^2$ area generally containing no more than three microcalcifications (MA et al., 2010).

This work aims to develop a computer vision system to detect microcalcifications in mammographic images, using images from the Curated Breast Imaging Subset of Digital Database for Screening Mammography (CBIS-DDSM) database. The detection algorithm is divided into two parts: pre-processing and segmentation. A region of interest was not defined, as it is considered that the entire breast is subject to the appearance of microcalcifications. The idea here is to compare it with other works in the same context. Therefore, this work presents a proposal for a method for detecting microcalcifications in mammography using image processing, which is of great importance in the health area.

The remainder of this paper is organized as follows. In Section 2, some related work is discussed. Section 3 describes the methodology used. Section 4 addresses the performance evaluation methodology. Section 5 presents the results obtained, and Section 6 presents the conclusions of this paper.

2 Related Work

This section analyzes some related work with the aim of exploring the latest research focusing on the detection of microcalcifications in Mammography images.

Hernández-Capistrán, Martínez-Carballido e Rosas-Romero (2018) developed an algorithm that detects microcalcifications in Mammography images using morphological processing, machine learning, and some feature considerations. His work achieved an accuracy rate above 97%. Chen et al. (2014) estimated the connectivity between groups of microcalcifications using morphological dilation and multiple scales. A classifier

of microcalcification groups into malignant and benign was developed using morphological feature extraction.

The work of Dong et al. (2015) performs image preprocessing, segmentation, and feature extraction and uses variations of the Support Vector Machine (SVM) technique to classify Mammography images. The proposed approach achieved % accuracy of 97.73%, using the Digital Database for Screening Mammography (DDSM) database. Gowri, Valluvan e Chamundeeswari (2018) developed a classifier using Multilayer Perceptron Neural Networks to classify microcalcifications as malignant or benign. To this end, images were pre-processed with attribute extraction.

Kamra et al. (2016) studied the effects of having a region of interest (ROI) of fixed and variable size on the classification of Mammography images. To evaluate the algorithm's performance in various situations, kernels using SVM were used. The objective of the work developed by Rosa et al. (2015) is to use the Muliple-Instance Learning (MIL) algorithm to diagnose breast cancer specialists. Selvi e Suganthi (2018) developed an improved adaptive gray scaling method for breast cancer prediction, the gray level covariance matrix (GLCM). The proposed algorithm achieved 99% accuracy and less computation time in terms of classification.

Sert, Ertekin e Halici (2017) developed an algorithm that performs data cleaning, removes arbitrary image deformations that appear at the edges, and uses data augmentation techniques. This algorithm was trained and tested using six different pre-processing approachesand ninet set combinations. Each model is trained for 50,000 iterations, achieving an accuracy of 94.3%. Sabherwal, Agrawal e Singh (2017) proposed an algorithm that automatically removes artifacts, labels, and pectoral muscles and suppresses noise without human intervention. Utilizes Gray-Level Co-Occurrence Matrix (GLCM) contrast, where this segmentation approach relies on improving region growth to preserve boundary information. This method showed an accuracy of 66.65%.

Zhang et al. (2014) uses gamma correction and a double structural element based on a mathematical morphology to improve microcalcifications. Top-hat transformation is also used to suppress the background. The double threshold technique is used to detect the potential region of microcalcification. The shapes and statistical characteristics of each microcalcification identified by detection are extracted and fed into the SVM to reduce the number of false positives, thus obtaining 92.07% accuracy.

Considering that none of the articles mentioned above uses a Self Organized Map (SOM) neural network, this work proposes its use to evaluate and compare results.

3 Methodology

The proposed work is divided into two parts, image preprocessing and segmentation, the process as a whole is represented through a flowchart presented later. A region of interest (ROI) was not defined, as it is considered that the entire breast is subject to the appearance of microcalcifications. All 20 images diagnosed with malignant cancer from the Curated Breast Imaging Subset of Digital Database for Screening Mammography (CBIS-DDSM) database were subjected to a pre-processing and segmentation algorithm. This number of images was sufficient for training the algorithm. The programming language used was Python, together with the Numpy (IDRIS, 2015; BLOICE; HOLZINGER, 2016; BRESSERT, 2012) and OpenCV (MORDVINTSEV; ABID, 2013) libraries.

Figure 2 presents a complete flowchart of the process methodology for obtaining results.

3.1 Data Base

The database used in this work is the CBIS-DDSM (Curated Breast Imaging Subset of DDSM), an update of the standardized version of the DDSM (Digital Database for Screening Mammography). This database contains 2620 studied Mammography images, with a variety of diagnoses, including normal, malignant, and benign. Validation of this database makes it a valuable tool in developing and testing decision support systems. As part of the database update, images were decompressed and converted to DICOM format, bounding boxes and region of interest (ROI) segmentation were updated, and pathological diagnosis for training data was also included (LEE et al., 2017). For this work, 20 Mammography images were used, all with malignant cancer, to develop an algorithm that detects microcalcifications to compare with the gold standard diagnosed by specialists.

3.2 Gamma Correction of the Original Mammography

Gamma correction is a non-linear contrast adjustment that improves the highlight of brighter pixels or vice

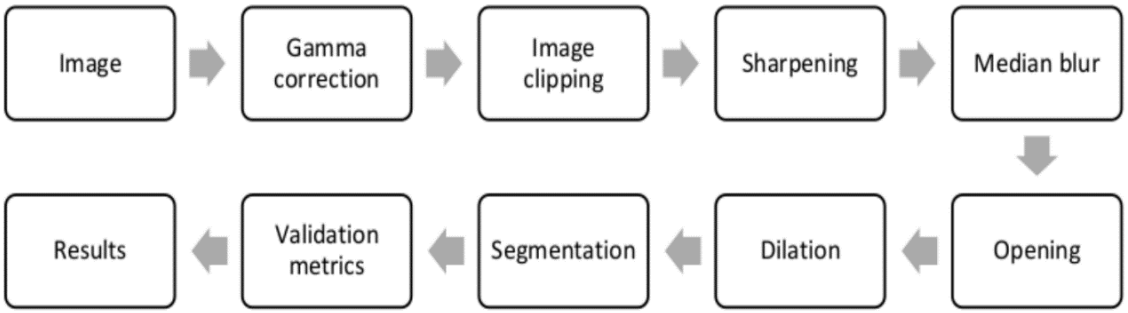

Figure 2: Complete flowchart of the process methodology.

versa. This correction is used to improve the overall lower contrast of the image as

$$F(x, y) = (I(x, y))^{\frac{1}{\gamma}}, \tag{1}$$

where $I(x, y)$ represents the original mammography image, $F(x, y)$ enotes the enhanced mammography image obtained through gamma correction and γ is the gamma value used for enhancement.

Figure 3 shows a section of the region containing microcalcifications in Figure 1 and its result after applying gamma correction. In Figure 3a there is the original Mammography image and in Figure 3b the image after gamma correction. It is clear that this method enhances the contrast of the image, and microcalcifications can be more easily identified.

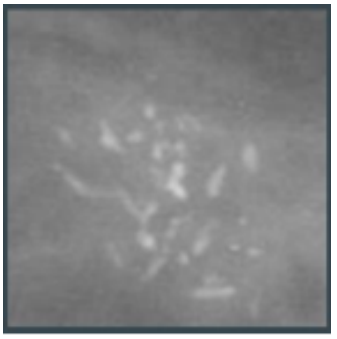

(a) Original Mammography image.

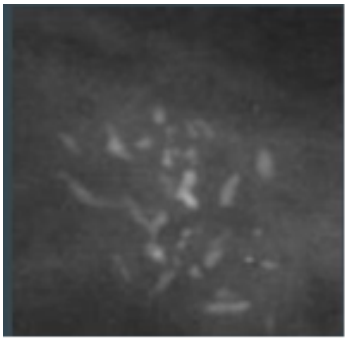

(b) Image post gamma correction.

Figure 3: Gamma correction.

3.3 Image Clippings

After gamma correction, each Mammography image is divided into multiple 120×120 pixel parts to facilitate pre-processing. This step is necessary due to the large size of the original images. Each cut goes through a repeat loop to traverse the image vertically and horizontally in order to carry out the next pre-processing and segmentation steps.

3.4 Opening (Dilation and Erosion)

Dilation and erosion are morphological processing tools. The basic effect of Opening is somewhat similar to erosion in that it tends to remove some of the foreground (bright) pixels from the edges of the foreground pixel regions. However, it is less destructive than erosion in general. As with other morphological operators, the exact operation is determined by a structuring element. The effect of the operator is to preserve foreground regions that have a similar shape to this structuring lement, or that may completely contain the structuring lement, while eliminating all other foreground pixel regions (GONZALEZ; WOODS, 2009).

The result of this step is sin the Figure 4. Figure 4a shows the image after gamma correction, and Figure 4b the image after opening processing.

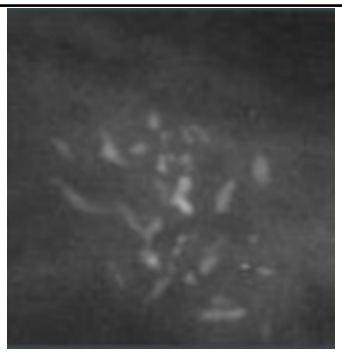

(a) Image after gamma correction.

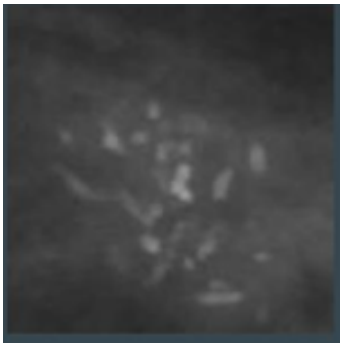

(b) Image after opening processing.

Figure 4: Opening processing.

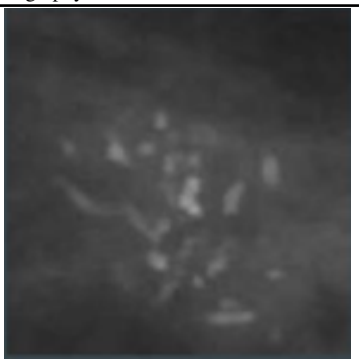

(a) Opening post processing image.

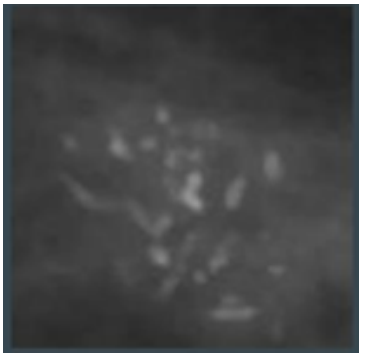

(b) Median Blur post-processing image.

Figure 5: Median Blur processing.

3.5 Median Blur

The Median Blur function calculates the median of all pixels under the kernel window, and the center pixel is replaced with this median value. This is highly effective in removing salt and pepper noise. An interesting thing to note is that in Gaussian and box filters, the filtered value for the central element can be a value that may not exist in the original image. However, this is not the case in median fitering, since the central element is always replaced by some pixel value in the image. This reduces noise effectively. The kernel size must be a positive odd integer, for this work the kernel is 5 (MORDVINTSEV; ABID, 2013).

The result of this step is seen in the Figure 5. Figure 5a shows the opost-processingcessing image, and Figure 5b the Median Blur post-processing image.

3.6 Sharpening

Applying the sharpening or sharpening filter sharpens the edges of the image. This filbeneficial useful when you want to improve the edges in an image that is not sharp. The level of sharpness depends on the type of kernel that is used (SINGH; SRIVASTAVA; SRIVASTAVA, 2018).

There are multiple configuration options for the kernel in image processing, each offering distinct effects on the sharpness of the image. Kernels are matrices applied to an image through convolution, where the values in the kernel determine how the surrounding pixels influence the sharpening effect.

For this work, the chosen kernel is

$$K = \begin{bmatrix} -1 & -1 & -1 \\ -1 & 9 & -1 \\ -1 & -1 & -1 \end{bmatrix}. \tag{2}$$

This specific kernel enhances the sharpness of an image by amplifying the intensity of the central pixel (with a weight of 9) relative to its neighbors (each with a weight of -1). During convolution, the kernel emphasizes the contrast between the central pixel and its surrounding pixels, effectively highlighting edges and fine details in the image. This approach is particpractical-

fective for enhancing the clarity of mammography images by making subtle features more distinguishable.

The Figure 6 shows the Sharpening processing. Figure 6a shows thepost-processingcessing Median Blur, and Figure 6bpost-processingcessing Sharpening.

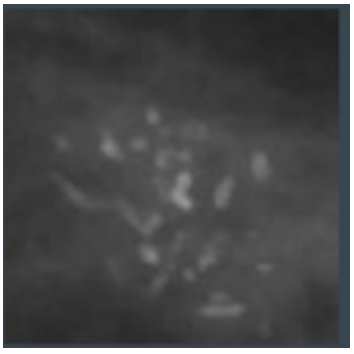

(a) post-processing Median Blur.

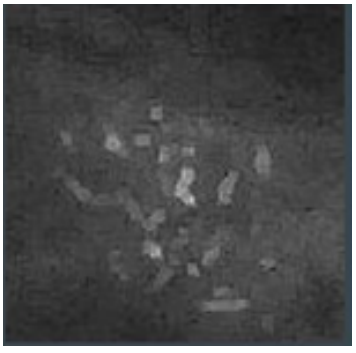

(b) post-processing Sharpening

Figure 6: Sharpening processing.

3.7 Dilatation

The difference between this step and the one processed in Subsection 3.4 is that only dilation is used here, which is the enlargement of objects in a binary The shape of the structuring element controls the specific shape and extent of this spacing element used (GONZALEZ; WOODS, 2009). The kernel size for this work wa

The Figure 7 shows the image through dilation. Figure 7a shows the post-processing sharpening, and Figure 7b shows the post-processing dilation.

(a) post-processing Sharpening.

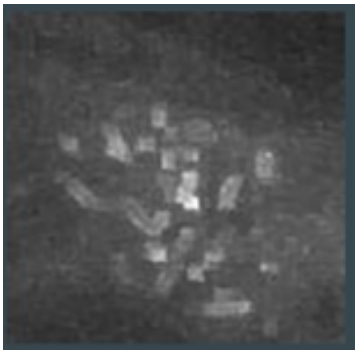

(b) Dilation post-processing image.

Figure 7: Dilatation processing.

3.8 Segmentation

The purpose of segmenting Mammoimagesy image is to highlight microcalcifications, which are almost imperceptible when seen in the original image. Image segmentation was performed in tw: stself-organizing maping Map (SOM) neural network and a threshold filter.

SOM is an unsupervised learning neural network. Its system is based on competitive learning. There is a competition between neurons to be activated (winner). The SOM network can be implemented by having connections with lateral inhibitions, that is, the winner neuron's ability to reduce its neighbors' activity by giving them negative feedback. There is also the concept of a topographic map, where some neighboring neurons represent the information generated from an input and has an interaction of short connections (GRECO et al., 2024).

Points in the input data space have corresponding points in the output space. The weights are initialized with random values. Then, all neurons calculate the discrimination function, presented in Equation 3, on the characteristics of the database. The neuron with the

lowest value is considered the champion, that is,

$$D_j(x) = \sum_{i=1}^{D}(x_i - w_{ji})^2. \quad (3)$$

Neighboring neurons to the activated one will be more excited than those further away. This process is called topological neighborhood and is calculated as

$$T_{j,I(x)} = exp(\frac{-S^2_{j,I(x)}}{2\sigma^2}), \quad (4)$$

where S is the lateral distance between neurons, $I(x)$ is the winner neuron index and σ is the number of neighbors that decreases over time. The topographic neighborhood will be tending to zero when a neuron is very far from the winner.

With t being the number of epochs and $\eta(t)$ the learning rate over time, the weights are updated as shown

$$\Delta w_{ij} = \eta(t)T_{j,I(x)}(t)(x_i - w_{ji}) \quad (5)$$

The weights are moved according to the topological neighborhood. This produces an effect as if the winning neuron attracts the other neurons (YU et al., 2023). For this work, the SOM network divides the mammography image into clusters based on pixel neighborhood characteristics. The image is divided into just nine intensities of gray tones, as shown in Figure 8. Figure 8a shows the image post-processing Sharpening and Figure 8b segmented image.

The threshold filter plays a fundamental role after the SOM network divides the imagnine into 9 shades of gray. It then divides the background (8 gray intensities) from the microcalcification threshold intensity,y, i.e. the whitest intensity. There are 16 bits (0-65535), the threshold used is greater than or equal to 40500. Figure 9 shows the image after going through the segmentation process. The following figure shows an example of a region that presents microcalcifications going through all pre-processing and segmentation steps.

(a) post-processing Sharpening.

(b) Segmented image.

Figure 8: Segmentation processing.

4 Performance Assessment Methodology

After applying the pre-processing and segmentation techniques, the microcalcifications are displayed in white in a binarized image. The entire backisontains whichk, this serves to highlight the microcalcifications. A white rectangle is drawn in the region containing microcalcifications to be compared wiarea region marked by radiologists specialized in detecting them, the gold standard, as shown in Figure 10. Gold standard information is included in the CBIS-DDSM database.

Some performance evaluation techniques are used to validate the work. Accuracy, observed in Eq. (6), measures the proportion of correct predictions, without considering what is positive and what is negative. Sensitivity, Eq. (7), gives the proportion of true positives. Specificity, Eq. (8) is the proportion of true negatives. Positive predictive value, Eq. vpp, proportion of true positives about all positive predictions. Similarity Dice, Eq. (10), which compares how much areas overlap with others. These equations, in isolation, are susceptible to imbalances in the data set and can easily lead to the wrong conclusion about the system's performance. The equations are

$$Accuracy = \frac{(VP + VN)}{(P + N)}, \quad (6)$$

$$Sensitivity = \frac{VP}{VP + FN)}, \quad (7)$$

$$Specificity = \frac{VN}{(VN + FP)}, \quad (8)$$

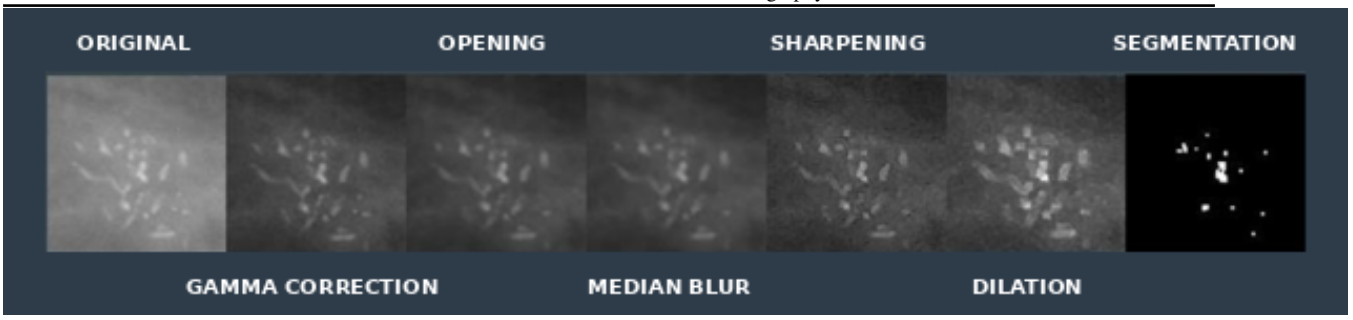

Figure 9: Region with microcalcification undergoing all pre-processing and segmentation steps.

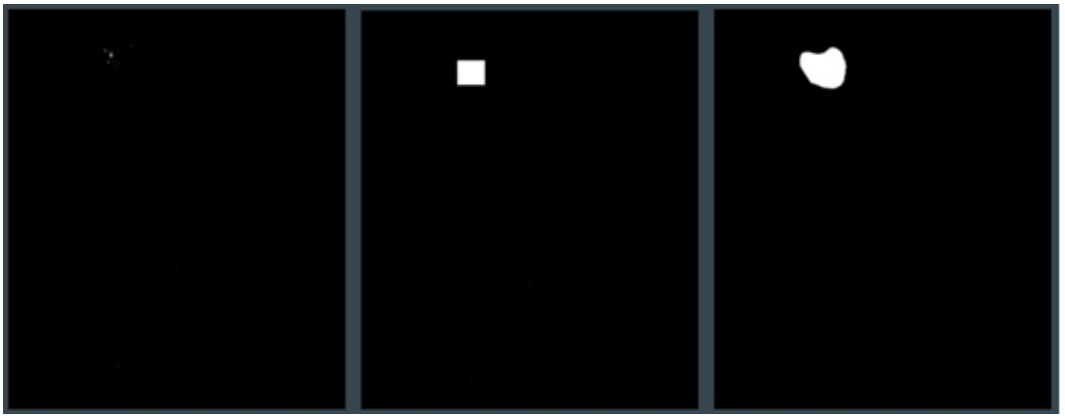

Figure 10: process used for system performance assessments.

$$Positivepredictivevalue = \frac{VP}{(VP + FP)}, \quad (9)$$

$$DiceSimilarity = \frac{2C}{A + B}, \quad (10)$$

where VP is true positive, VN is true negative, P is total positives, N is total negatives, FN is false negative, FP is false positive, A is segmented image area, the B is gold standard area, and the C is sum of the areas shared by the two images.

5 Results

This section presents the research results with the proposed method for detecting microcalcifications in mammography using image processing.

Experimental analyses were developed to evaluate the proposed method using the CBIS-DDSM database using the Python language and the Numpy and OpenCV libraries. To identify microcalcifications in Mammography images, experiments show that the accuracy of the method is 98.2%, the sensitivity is 49.6%, the specificity is 89.3%, the positive predictive value is 78.7% and Dice Similarity is 52.7%.

Table 1 presents the experimental results of the Mammography image of the proposed method, in summary form, of the accuracy, sensitivity, specificity, positive predictive value, and Dice similarity.

The proposed work presents greater accuracy than that of all related works researched, by the number of images used, howevemethod's effectiveness method should not be considered solely through isolated evaluation techniques. These eq,uations in is,olation are susceptible to imbalances in the data set and can easily lead to the wrong conclusion about the system's performance. Table 2 below shows a comparison between this work and other recent related works, where the works (authors), number of images, database, and accuracy are presented.

As shown in Table 2, the proposal presented here presented an accuracy of 98.2% with 20 images from the databaseCompared to other studies, the accuracy wasas only lower than the work by Selvi et al. (SELVI; SUGANTHI, 2018). We can state that the technique

Table 1: Results obtained in the research for the proposed method.

Num. of images	Database	Accuracy	Sensitivity	Specificity	True positive	Dice similarity
20	CBIS-DDSM	98.2%	49.6%	89.3%	78.7%	52.7%

Table 2: Comparative table between this work and other related works.

Work	Number of images	Database	Accuracy
Proposed	20	CBIS-DDSM	98.2%
Gowri et al	50	MIAS	96.3%
Chen et al.	20, 25	MIAS, DDSM	96.0%
Selvi et al.	130	MIAS	99.5%
Kamra et al.	140	MIAS, IRMA E ACE	95.34%

used here can detect microcalcifications in mammography using digital image processing.

A database similar to that of the researched works was used to compose the research base, however, the sample of 20 Mammography image used in this work is small compared to the others.

The objective of this work was to detect microcalcifications in Mammography image images. The research studies go beyond this scodiagnoseosis of malignant or benign cancer. To achieve this, several characteristics of microcalcifications must be considered. These characteristics must then be used as an input base for some algoriclassifyication.

It can also be stated here that the work presents an important contribution in the area of health, as it proposes a method for detecting microcalcifications in mammography using image processing, which can be used to help diagnose anddncer to determine whether it is malignant or benign.

6 Conclusions

The accuracy of the method, 98.2%, attests to the system's good performance. Additionally, the specificity of 89.3% indicates a satisfactory ability to correctly predict the absence of the condition when it is truly not present. The positive predictive value of 78.7% demonstrates the algorithm's reasonable capability to correctly identify positive cases. However, the sensitivity of 49.6% highlights room for improvement, as nearly half of the positive cases were not correctly detected. The Dice Similarity metric of 52.7% reinforces this observation, indicating a challenge in the precise segmentation of microcalcifications.

The main contribution of this work lies in applying computer vision techniques for detecting microcalcifications in mammographic images, utilizing digital image processing. The developed method can serve as a diagnostic aid for radiologists, assisting healthcare professionals in the early identification of potential lesions.

As a proposal for future work, the aim is to enhance the detection system by increasing the method's sensitivity to reduce the false negative rate. Additionally, it is suggested to implement a computer vision system capable of classifying microcalcifications as benign or malignant, expanding the approach's applicability for more precise diagnostic support. Therefore, there is a vast field of research to be explored at the intersection of artificial intelligence and healthcare, aiming for continuous improvements in detecting and classifying mammographic abnormalities.

Acknowledgments

ARA thanks the National Research Council - CNPq through call 305359/2021-5 and 442182/2023-6, the Internal Simplified Call PRPI/Postgraduate - Grant Support for IFCE Stricto Sensu Postgraduate Programs, FUNCAP (UNI-0210-00699.01.00/23 e Edital 38/2022), and the Brazilian Federal Agency for Support and Evaluation of Graduate Education - CAPES.

References

BLOICE, M. D.; HOLZINGER, A. A tutorial on machine learning and data science tools with python. **Machine Learning for Health Informatics: State-of-the-Art and Future Challenges**, Springer, p. 435–480, 2016.

BRESSERT, E. Scipy and numpy: an overview for developers. "O'Reilly Media, Inc.", 2012.

CHEN, Z.; STRANGE, H.; OLIVER, A.; DENTON, E. R.; BOGGIS, C.; ZWIGGELAAR, R. Topological modeling and classification of mammographic microcalcification clusters. **IEEE transactions on biomedical engineering**, IEEE, v. 62, n. 4, p. 1203–1214, 2014.

DIKICI, E.; BIGELOW, M.; PREVEDELLO, L. M.; WHITE, R. D.; ERDAL, B. S. Integrating ai into radiology workflow: levels of research, production, and feedback maturity. **Journal of Medical Imaging**, Society of Photo-Optical Instrumentation Engineers, v. 7, n. 1, p. 016502–016502, 2020.

DOI, K. Computer-aided diagnosis in medical imaging: historical review, current status and future potential. **Computerized medical imaging and graphics**, Elsevier, v. 31, n. 4-5, p. 198–211, 2007.

DONG, M.; LU, X.; MA, Y.; GUO, Y.; MA, Y.; WANG, K. An efficient approach for automated mass segmentation and classification in mammograms. **Journal of digital imaging**, Springer, v. 28, p. 613–625, 2015.

GONZALEZ, R. C.; WOODS, R. C. **Processamento digital de imagens .** [S.l.]: Pearson Educación, 2009.

GOWRI, V.; VALLUVAN, K.; CHAMUNDEESWARI, V. V. Automated detection and classification of microcalcification clusters with enhanced preprocessing and fractal analysis. **Asian Pacific Journal of Cancer Prevention: APJCP**, Shahid Beheshti University of Medical Sciences, v. 19, n. 11, p. 3093, 2018.

GRECO, M.; GIARNETTI, S.; GIOVENALE, E.; TASCHIN, A.; LECCESE, F.; DORIA, A.; SENNI, L. Thz data analysis and self-organizing map (som) for the quality assessment of hazelnuts. **Applied Sciences**, MDPI, v. 14, n. 4, p. 1555, 2024.

HERNÁNDEZ-CAPISTRÁN, J.; MARTÍNEZ-CARBALLIDO, J. F.; ROSAS-ROMERO, R. False positive reduction by an annular model as a set of few features for microcalcification detection to assist early diagnosis of breast cancer. **Journal of Medical Systems**, Springer, v. 42, p. 1–9, 2018.

IDRIS, I. **NumPy: Beginner's Guide**. [S.l.]: Packt Publishing Ltd, 2015.

JEMAL, A.; BRAY, F.; CENTER, M. M.; FERLAY, J.; WARD, E.; FORMAN, D. Global cancer statistics. **CA: a cancer journal for clinicians**, Wiley Online Library, v. 61, n. 2, p. 69–90, 2011.

KAMRA, A.; JAIN, V.; SINGH, S.; MITTAL, S. Characterization of architectural distortion in mammograms based on texture analysis using support vector machine classifier with clinical evaluation. **Journal of digital imaging**, Springer, v. 29, p. 104–114, 2016.

LEE, R. S.; GIMENEZ, F.; HOOGI, A.; MIYAKE, K. K.; GOROVOY, M.; RUBIN, D. L. A curated mammography data set for use in computer-aided detection and diagnosis research. **Scientific data**, Nature Publishing Group, v. 4, n. 1, p. 1–9, 2017.

LI, Q.; NISHIKAWA, R. M. **Computer-aided detection and diagnosis in medical imaging**. [S.l.]: Taylor & Francis, 2015.

LITJENS, G.; KOOI, T.; BEJNORDI, B. E.; SETIO, A. A. A.; CIOMPI, F.; GHAFOORIAN, M.; LAAK, J. A. V. D.; GINNEKEN, B. V.; SÁNCHEZ, C. I. A survey on deep learning in medical image analysis. **Medical image analysis**, Elsevier, v. 42, p. 60–88, 2017.

MA, Y.; TAY, P. C.; ADAMS, R. D.; ZHANG, J. Z. A novel shape feature to classify microcalcifications. In: IEEE. **2010 IEEE International Conference on Image Processing**. [S.l.], 2010. p. 2265–2268.

METZGER-FILHO, O.; TUTT, A.; AZAMBUJA, E. D.; SAINI, K. S.; VIALE, G.; LOI, S.; BRADBURY, I.; BLISS, J. M.; JR, H. A. A.; ELLIS, P. et al. Dissecting the heterogeneity of triple-negative breast cancer. **Journal of clinical oncology**, American Society of Clinical Oncology, v. 30, n. 15, p. 1879–1887, 2012.

MLADOVSKY, P. **Health in the European Union: trends and analysis**. [S.l.]: WHO Regional Office Europe, 2009.

MORDVINTSEV, A.; ABID, K. Opencv-python tutorials. **Obtenido de https://opencvpythontutroals. readthedocs. io/en/latest/py_tutorials/py_imgproc/py_table_of_contents_imgproc/py_table_of_contents_imgproc. html**, 2013.

NETWORK, N. C. C. et al. Nccn clinical practice guidelines in oncology^< tm>: breast cancer. **http://www. nccn. org**, 2007.

ROSA, R. S. de la; LAMARD, M.; CAZUGUEL, G.; COATRIEUX, G.; COZIC, M.; QUELLEC, G. Multiple-instance learning for breast cancer detection in mammograms. In: IEEE. **2015 37th Annual International Conference of the IEEE Engineering in Medicine and Biology Society (EMBC)**. [S.l.], 2015. p. 7055–7058.

SABHERWAL, P.; AGRAWAL, M.; SINGH, L. Automatic detection of the r peaks in single-lead ecg signal. **Circuits, Systems, and Signal Processing**, Springer, v. 36, p. 4637–4652, 2017.

SELVI, C.; SUGANTHI, M. A novel enhanced gray scale adaptive method for prediction of breast cancer. **Journal of medical systems**, Springer, v. 42, n. 11, p. 221, 2018.

SERT, E.; ERTEKIN, S.; HALICI, U. Ensemble of convolutional neural networks for classification of breast microcalcification from mammograms. In: IEEE. **2017 39th Annual International Conference of the IEEE Engineering in Medicine and Biology Society (EMBC)**. [S.l.], 2017. p. 689–692.

SHEN, L.; RANGAYYAN, R. M.; DESAUTELS, J. L. Application of shape analysis to mammographic calcifications. **IEEE transactions on medical imaging**, IEEE, v. 13, n. 2, p. 263–274, 1994.

SICKLES, E. A. Breast calcifications: mammographic evaluation. **Radiology**, v. 160, n. 2, p. 289–293, 1986.

SINGH, V. P.; SRIVASTAVA, S.; SRIVASTAVA, R. Automated and effective content-based image retrieval for digital mammography. **Journal of X-ray Science and Technology**, IOS Press, v. 26, n. 1, p. 29–49, 2018.

SOCIETY, A. C. **Breast cancer facts & figures**. [S.l.]: American Cancer Society, 2007.

YU, A.; LIU, X.; FU, F.; CHEN, X.; ZHANG, Y. Acoustic emission signal denoising of bridge structures using som neural network machine learning. **Journal of Performance of Constructed Facilities**, American Society of Civil Engineers, v. 37, n. 1, p. 04022066, 2023.

ZHANG, X.-S. et al. A new approach for clustered mcs classification with sparse features learning and twsvm. **The Scientific World Journal**, Hindawi, v. 2014, 2014.